

Real-time monitoring and diagnosis of photovoltaic system degradation only using maximum power point—the Suns-V_{mp} method

Xingshu Sun  | Raghu Vamsi Krishna Chavali  | Muhammad Ashraful Alam

Network of Photovoltaic Technology, Purdue University, West Lafayette, IN 47907, USA

Correspondence

Xingshu Sun, Network of Photovoltaic Technology, Purdue University, West Lafayette, IN 47907, USA.
Email: sun106@purdue.edu

Funding information

National Science Foundation, Grant/Award Numbers: #1724728 and 1724728; US-India Partnership to Advance Clean Energy-Research (PACE-R) for the Solar Energy Research Institute for India and the United States (SERIUS)

Abstract

The uncertainties associated with technology-specific and geography-specific degradation rates make it difficult to calculate the levelized cost of energy, and thus the economic viability of solar energy. In this regard, millions of fielded photovoltaic modules may serve as a global testbed, where we can interpret the routinely collected time series maximum power point (MPP) data to assess the time-dependent “health” of solar modules. The existing characterization methods, however, cannot effectively mine/decode these datasets to identify various degradation pathways. In this paper, we propose a new methodology called the *Suns-V_{mp} method*, which offers a simple yet powerful approach to monitoring and diagnosing time-dependent degradation of solar modules by using the MPP data. The algorithm reconstructs “IV” curves by using the natural illumination-dependent and temperature-dependent daily MPP characteristics as constraints to fit physics-based circuit models. These synthetic IV characteristics are then used to determine the time-dependent evolution of circuit parameters (eg, series resistance), which in turn allows one to deduce the dominant degradation modes (eg, solder bond failure) of solar modules. The proposed method has been applied to a test facility at the National Renewable Energy Laboratory. Our analysis indicates that the solar modules degraded at a rate of ~0.7%/year because of discoloration and weakened solder bonds. These conclusions are validated by independent outdoor IV measurements and on-site imaging characterization. Integrated with physics-based degradation models or machine learning algorithms, the method can also serve to predict the lifetime of photovoltaic systems.

KEYWORDS

reliability, maximum power point, field data, characterization, system level

1 | INTRODUCTION

As an alternative renewable energy resource, photovoltaics (PV) has experienced exponential growth over the last several decades. For investors, an important metric to benchmark the financial viability of PV against other energy resources is the levelized cost of electricity (LCOE). However, the current estimates of the LCOE for PV often rely on the presumption of a linear performance degradation rate over time. Unfortunately, this presumption leads to an inaccurate LCOE because some PV degradation processes are inherently nonlinear.¹

Also, the rate and magnitude of PV degradation depend sensitively on cell technology and vary substantially across geographic locations.^{2,3} Hence, a “technology-agnostic” monitoring method—that characterizes the temporal PV degradation in real time while taking the meteorological information into account—can improve our understanding of these technology-specific and location-specific degradation processes. This will improve LCOE estimates and suggest opportunities for reliability-aware design.

There have been many studies on PV reliability reported in the literature, based on different characterization methodologies. These

methodologies can be roughly divided into 2 groups: online vs off-line techniques. The online techniques include DC/G_{POA} , performance ratio (PR), photovoltaics for utility-scale applications, and machine learning. The off-line techniques involve IV measurements, advanced imaging techniques, material characterization, the Suns-Voc method, etc.

Online techniques rely on information routinely collected from solar modules. For example, Belluardo et al⁴ and Jordan and Kurtz⁵ have analyzed the online temporal evolution of PV degradation by continuously examining 3 time series performance metrics:

- (a) DC/G_{POA} is the ratio of temperature-corrected DC power over the plane-of-array irradiance.⁶
- (b) Performance ratio method ($PR = Y_G/Y_R$) uses the ratio of the generated output energy (Y_G) and the nameplate rating-based reference output energy (Y_R) to determine the degradation of a module.⁷
- (c) Finally, the photovoltaics for utility-scale application method uses linear regression to translate real-time output power to values at the standard test condition (STC) as a function of irradiance, ambient temperature, and wind speed.⁸

These methods have the advantage of calculating real-time STC efficiencies and degradation rates without disconnecting/interrupting the operation of solar modules. The understanding of degradation pathways, which is critical to establish the fundamental physics of PV degradation and promote reliability-aware design, is still missing from these analyses. As a result, another online characterization approach—that can potentially identify degradation pathways from field data by machine learning algorithms—has gained attention^{9–12}.

- (d) Machine learning has been proved to be a potent tool to analyze massive data and generate useful insights for different applications. It can potentially provide valuable information on PV degradation by various statistical analyses (eg, regression, classification, clustering). Nonetheless, the parameters in these algorithms are not physically defined, and therefore are generally difficult to interpret. Moreover, training the algorithms necessitates a tremendous amount of field data spanning across different geographic locations and technologies as training sets, which are not easily accessible.

On the other hand, off-line techniques examine the temporal degradation by periodically and temporarily disconnecting solar modules for detailed characterization. Thus, off-line techniques can easily diagnose the primary degradation pathways of fielded solar modules. Typical off-line techniques include the following:

- (a) By fitting the I-V characteristics by the double-diode model and then physically interpreting the extracted circuit parameters,¹³ Jordan et al were able to attribute the efficiency loss of the analyzed solar modules to the increased series resistance and recombination current.¹⁴ Sutterlueli et al also applied the empirical loss factors model¹⁵ to analyze the IV data of degraded solar modules, and ascribe the performance erosion to the deteriorated series and shunt resistances.¹⁶

- (b) Imaging techniques can yield spatially resolved information regarding degraded solar modules and enable extraction of location-resolved parameters. For example, by applying the method proposed in Trupke et al,¹⁷ Peike et al have successfully deduced the degree and spatial distribution of metal finger corrosion in silicon solar cells based on electroluminescence and photoluminescence images.¹⁸
- (c) Material characterization techniques have also been used to study the fundamental mechanisms underlying PV degradation processes (eg, sodium migration of potential-induced degradation (PID) via transmission electron microscopy and energy-dispersive X-ray spectroscopy¹⁹).
- (d) The Suns-Voc method monitors the open-circuit voltage while manually varying illumination intensity of a solar simulator (see Figure 1).²⁰ Jordan et al have applied this method to extract photocarrier lifetime and series resistance of degraded solar modules.¹⁴ In addition, this method can directly measure heterojunction-induced degradation in solar cells,^{21,22} something that other characterization methods cannot easily perform.

Indeed, these off-line methods are incredibly powerful for degradation characterization; however, they require interrupting the normal operation of solar modules at the maximum power point (MPP). Therefore, these techniques are not suitable for continuous monitoring. We have comprehensively summarized the relative merits of these techniques in Table S1 located in Sec. A of the supplementary information (SI).

Inspired by the Suns-Voc method, in this paper, we have developed a simple yet powerful strategy called the Suns-Vmp method, which combines the capabilities of both online and off-line techniques (ie, mine the real-time field data composed exclusively of MPP current (I_{mp}) and voltage (V_{mp}) to identify various degradation pathways). This Suns-Vmp method, by taking advantage of the natural daily variation of sunlight, can deduce circuit parameters as a function of time by fitting the reconstructed MPP "IV" throughout the day; see Figure 1. By systematically and physically mining the streaming MPP data, the method can monitor the reliability of solar modules in real time. The code to perform the Suns-Vmp method can be downloaded from Ref. 23.

In this paper, we begin by introducing the detailed methodology of the Suns-Vmp method in Section 2. In Section 3, the Suns-Vmp method is applied to a test facility at the National Renewable Energy Laboratory (NREL) to extract the degradation rate and the dominant degradation modes. Section 4 discusses the implications of the Suns-Vmp method on the prediction and design of PV reliability and the limitations herein. Finally, we summarize the paper in Section 5.

2 | THE SUNS-VMP METHOD

In this section, we will discuss the algorithm of the Suns-Vmp method, as summarized in Figure 2. The algorithm has the following 4 steps: (1) adopt the physics-based equivalent circuit model for a specific technology, (2) extract pristine (time zero) circuit parameters based on datasheet pre-installation IV characteristics, (3) preprocess MPP data to reconstruct IV characteristics synthetically, and finally (4) analyze

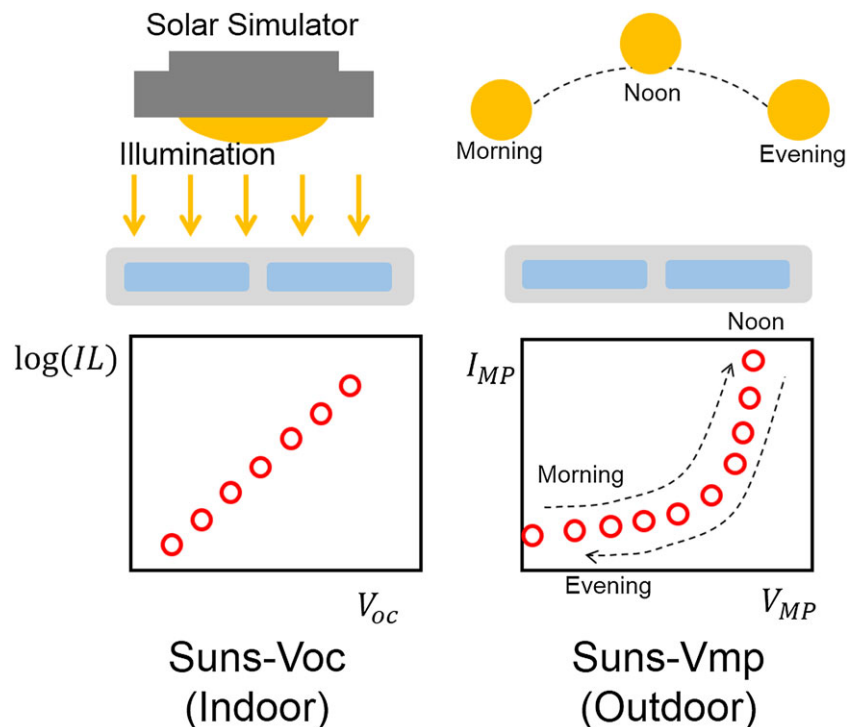
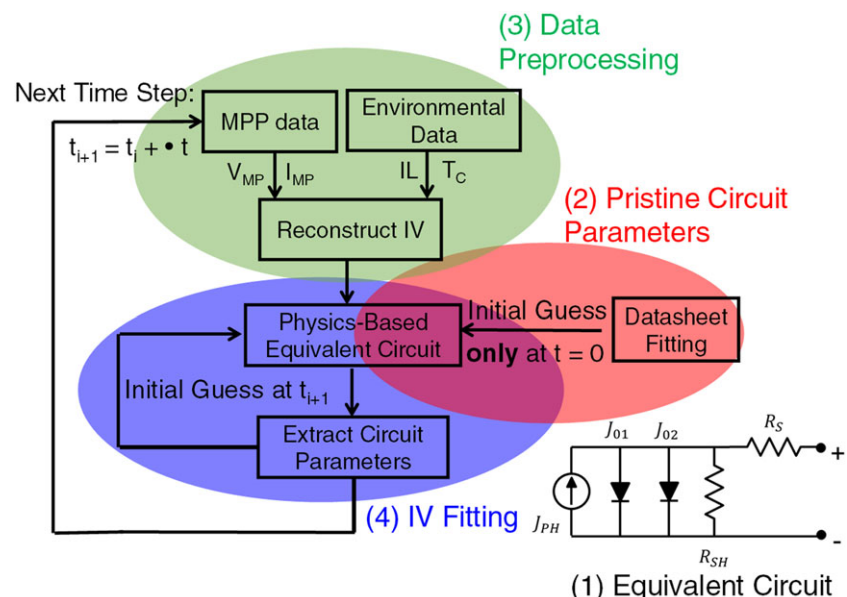


FIGURE 1 A schematic illustration to explain the working principles of the Suns-Voc and Suns-Vmp methods [Colour figure can be viewed at wileyonlinelibrary.com]

FIGURE 2 The flow chart of the Suns-Vmp method. The analytical formulation of the double-diode model is from Hejri et al¹³ and summarized in Sec. E of the SI. In the circuit diagram, J_{PH} is the maximum photocurrent density, J_{01} and J_{02} are the reverse saturation current densities with ideality factors of 1 and 2, respectively, R_{SH} is the shunt resistance, and R_S is the series resistance. Degradation mechanisms that affect the performance of solar modules are reflected in the time-dependent changes of these circuit parameters. For example, yellowing will reduce J_{PH} , and solder bond failure will increase R_S [Colour figure can be viewed at wileyonlinelibrary.com]



the temporal evolution of circuit parameters for insights regarding the dominant degradation modes. The detailed procedure of the algorithm (eg, filtering outliers and preprocessing environmental data) is summarized in Secs. B and C of the SI.

2.1 | Step 1: development and choice of the equivalent circuit (compact) model

Mainstream PV technologies can be categorized into 3 groups: (1) p-n homojunction (eg, c-Si and GaAs), (2) p-i-n junction (eg, a-Si and perovskites), and (3) p-n heterojunction (eg, CIGS and CdTe). Depending on a particular technology, we select the corresponding equivalent circuit in the Suns-Vmp method: for example, Sun et al²⁴

for CIGS, Sun et al²⁵ for perovskites, and Chavali²⁶ for silicon heterojunction. Because a solar cell is exposed to varying illumination intensities and temperatures, the equivalent circuit must be capable of describing the illumination-dependent and temperature-dependent IV curves.

In this paper, we will demonstrate the Suns-Vmp method on a c-Si PV system; therefore, we make use of the well-known double-diode model for Si solar modules,¹³ which explicitly accounts for the illumination and temperature dependencies of circuit parameters, namely, J_{PH} , J_{01} , J_{02} , R_{SH} , and R_S ; see Figure 2. Compared to the single-diode model, the double-diode model can distinguish between recombination current in the quasi-neutral vs space-charge regions, denoted by J_{01} and J_{02} , respectively. Therefore, the double-diode

model allows us to deconvolve different degradation mechanisms more physically. For instance, PID, which increases carrier recombination in the space-charge region, will only increase J_{02} but keep J_{01} unchanged.

The complete set of equations and parameter descriptions for the double diode are summarized in the SI. If needed, the double-diode model can be generalized to include nonlinear shunt resistance²⁷ and temperature-dependent and illumination-dependent series resistance.^{28,29}

2.2 | Step 2: extracting pristine module parameters

Next, we extract the pristine (time zero) circuit parameters (before the module is fielded) as robust initial guesses for the Suns-Vmp method. We do so by fitting the complete illumination-dependent and temperature-dependent IV measurements available from the datasheet or pre-installation measurement. With these robust initial guesses, we can eliminate multiple solutions in the sequential IV fitting process. Typical datasheets usually provide a set of full IV measurements under various illumination and temperature conditions. Fitting these multiple IV curves guarantees the uniqueness of the extracted circuit parameters and consequently the robustness of the initial guess; see Figure 3. In this paper, we have used the nonlinear least-squares fitting algorithm and bioinspired particle swarm optimization (PSO) ("lsqcurvefit" and "particleswarm" functions in MATLAB[®],³¹ respectively). Both methods give identical results.

2.3 | Step 3: preprocessing MPP data

Over the duration of onsite operation, we construct—at any time during the onsite operation—a synthetic IV curve by sampling MPP data over a given period (typically 2–3 days, referred as the measurement window hereafter). Recall that in the Suns-Voc measurement, one tracks the open-circuit voltage of solar cells by deliberately varying the intensity of the solar simulator, to construct the IV curve in the absence of series resistance. In the Suns-Vmp method, however, we take advantage of the natural temporal variation of the sunlight (the

plane-of-array irradiance: G_{POA}) and the cell temperature (T_C) to track MPP. Hence, because of the changing G_{POA} and T_C , the module outputs I_{mp} and V_{mp} (operating current and voltage at MPP, respectively) increase from morning to noon then decrease from noon to evening; see Figure 4A. If the data is recorded every 10 minutes of 8 diurnal hours over a 3-day measurement window, then 144 data points of 4 variables (ie, G_{POA} , T_C , I_{mp} , V_{mp}) are available to calculate the circuit parameters of the circuit model, namely, calibrating the circuit parameters until the MPP IV is reproduced as shown in Figure 4B. Note that the Suns-Vmp method does not interrupt the normal operation of PV systems by disconnecting the solar modules to measure their IV characteristics; thus, the technique allows characterization of solar modules in real-time operation.

In the Suns-Vmp method, to reduce uncertainties in the parameter extraction, we also explicitly preprocess the time series data to account for (1) cell-to-module temperature difference, (2) spectral mismatch between pyranometer and solar modules, and (3) reflection loss as a function of angle of incidence. Fortunately, the Sandia PV Array Performance Model (SAPM) provides a set of functions implemented in MATLAB[®] to preprocess the environmental data. We have summarized the specific preprocessing steps based on SAPM in Sec. B of the SI. Also, while the basic algorithm is easy to understand, it is important to realize that the (G_{POA} , T_C , I_{mp} , V_{mp}) may involve noisy or corrupted data, which must be rejected for a robust parameter extraction of the circuit model. Hence, we have developed a physics-based self-filtering algorithm to preprocess the data before fitting. Unlike empirical data filters that need manual intervention⁵ (ie, examine results with different cutoff thresholds of outliers), our physics-based filter will automatically identify the outliers based on the initial fitting results and then remove them for the final fitting (see Sec. C of the SI for more detail).

The measurement window of MPP data must be chosen judiciously such that it is long enough to contain sufficient illumination/temperature variations, but short enough such that the module does not degrade significantly within the window. The timescale of degradation processes is slow; therefore, the circuit parameters can be assumed to be constant over the course of a few days. Hence, the recommended measurement window of MPP data can be up several days (eg, 3 days in Figure 4), as long as there exists sufficient variation in illumination and temperature to reconstruct the MPP IV. In the case of catastrophic degradation (such as partial shading degradation in thin-film solar modules³²), the extracted circuit parameters become the average of pre-degradation and post-degradation values over time.

2.4 | Step 4: MPP IV fitting algorithm

After reconstructing MPP IV and preprocessing environmental data, we proceed with simulating the measured MPP data to extract circuit parameters. Fitting algorithms, such as the nonlinear least-squares fitting algorithm and PSO, require a lower bound and an upper bound of each circuit parameter at each time step. In our analysis, circuit parameters are assumed to degrade monotonically as a function of time (ie, no recovery) with a maximum degradation rate of 1%/day, except for the short-circuit current J_{Ph} . Hence, once the measurement window is specified, the upper and lower bounds can be determined.

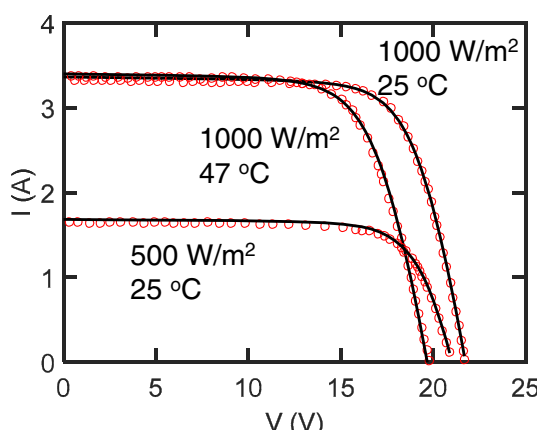
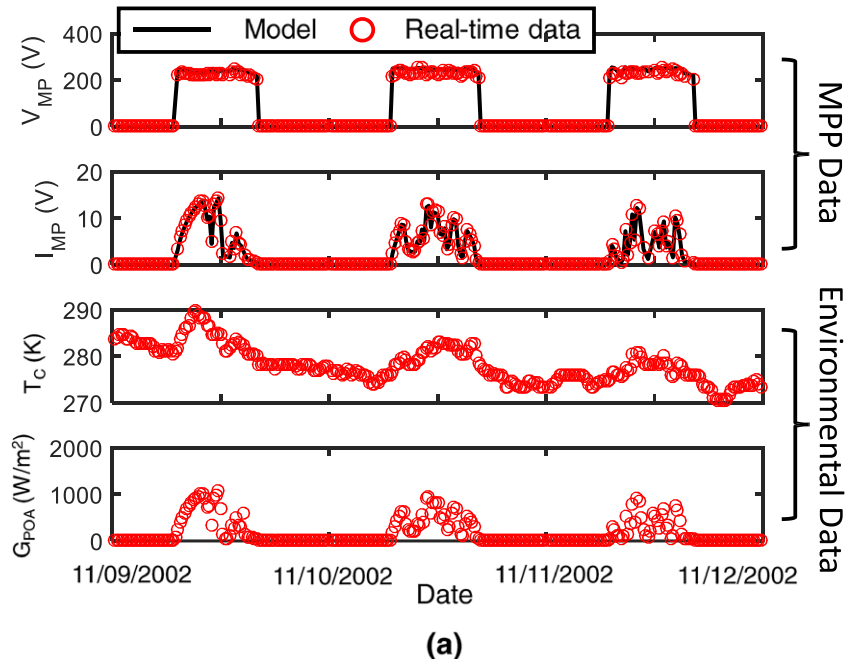
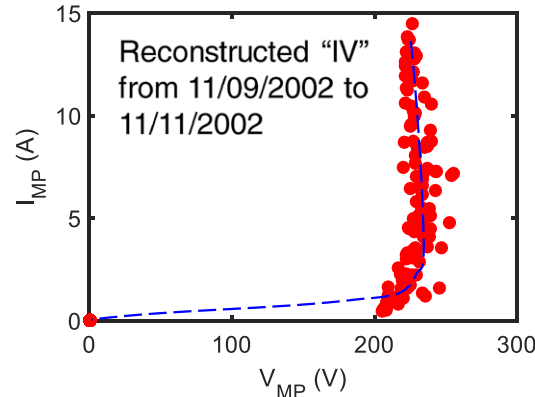


FIGURE 3 Initial fitting to the datasheet (Siemens M55³⁰) for time-zero circuit parameters. The extracted values of these circuit parameters are summarized in Sec. E of the SI [Colour figure can be viewed at wileyonlinelibrary.com]



(a)



(b)

FIGURE 4 A, Three-day maximum power point (MPP) and environmental data (circles) from November 09, 2002 to November 11, 2002 of the test facility in Sec. III. The fitting results of the MPP data (solid lines) using the Suns-Vmp method is also present. B, An illustration of reconstructing “IV” from the MPP data in (A) [Colour figure can be viewed at wileyonlinelibrary.com]

Because the short-circuit current may fluctuate significantly because of soiling and precipitation, the upper and lower bounds thereof are set to be the datasheet short-circuit current and zero, respectively. Even though recovery of certain degradation pathways is possible (eg, output power recovers after removing voltage stress for PID^{33,34}), such recovery is expected to be negligible because of constant environmental stress (eg, thermal cycling, moisture exposure) the solar modules is exposed to.

For any inverse modeling algorithm such as the Suns-Vmp method, one must ensure the uniqueness of the degradation analysis. Hence, we present a sensitivity analysis of these 2 algorithm parameters, ie, the measurement window and the maximum degradation rate of circuit parameters, on the final extraction of degradation rates; see Figure 5. Our results show that moderate change in the algorithm parameters in the Suns-Vmp method does not interfere with the final results—the deduced degradation rates of performance metric remain essentially unique.

In the next section, we will demonstrate the Suns-Vmp method on an NREL test facility with recorded field data to analyze the degradation of solar modules in real time. The analysis will reveal the possible root causes of power losses by physically interpreting the time-

dependent circuit parameters. The code and the field data used in this analysis can be downloaded from Sun et al²³.

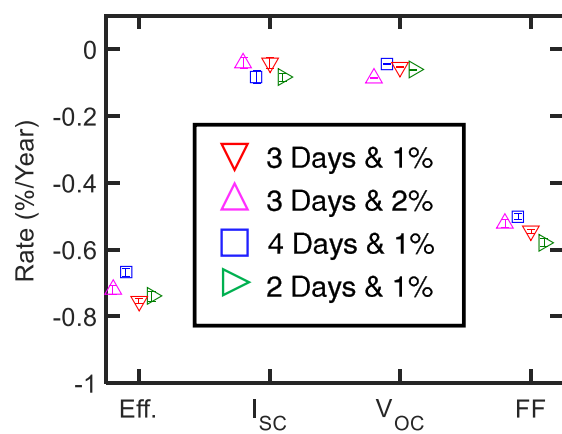


FIGURE 5 Degradation rate of performance metrics of the negative array as a function of different settings (ie, the measurement window and the maximum degradation rate of circuit parameters) in the Suns-Vmp method [Colour figure can be viewed at wileyonlinelibrary.com]

3 | APPLICATION TO FIELD DATA

3.1 | Introduction to field data

The studied PV system (No.: NREL x-Si #7) perches at the west side of the Solar Energy Research Facility building at NREL, Golden, CO, USA. It comprises 2 arrays with negative and positive monopoles, each of which consists of 5 strings with 14 x-Si Siemens M55 solar modules³⁰ totaling to around 7.42 kW capacity. In 2007, a negatively grounded inverter replaced the previous bipolar inverter, but we maintain the bipolar naming convention (negative versus positive) in this paper. The modules are 45° tilted and oriented 22° east of south. All the onsite MPP and environmental data (illumination and module temperature) including the metadata were retrieved from the publicly accessible NREL PV Data Acquisition database³⁵ with time resolution spanning from 1 to 15 minutes. The analyzed field data is from May 13, 1994 to December 31, 2014. Three thermocouples attached to the backsheet recorded the module temperature, but significantly, inconsistency was found after the eighth year. Therefore, we applied the calibrated Faiman model³⁶ to obtain module temperature. In addition to continuous MPP data, outdoor IV measurements were also carried out at the array level using a portable Daystar I-V tracer. These IV data sets help us validate the analysis obtained from the Suns-Vmp method. More details on this PV system can be found in Jordan et al.³⁷

Figure 6 displays 2 illustrative datasets, which highlights 2 major challenges of analyzing this PV system: (1) There are significant gaps up to 5 years in the field data, and (2) some of the data is corrupted, possibly because of instrumentation error, inverter clipping, weather condition, etc. First, to mitigate the uncertainty in deducing the circuit parameters induced by missing data, the Suns-Vmp method makes use of the results from the previous time step as initial guesses and establishes the upper/lower bounds with a preset maximum change rate when fitting the MPP IV. Second, we need a self-consistent scheme to detect and remove these outliers. Toward this goal, we have created a continuous physics-based self-filtering algorithm as summarized in the SI. Enabled by these techniques, the Suns-Vmp method can retain excellent error control, ie, the mean absolute percentage error is less than 5% for both Vmp and Imp throughout the entire 20-year analysis.

3.2 | Results and validation

Figure 7 summarizes the extracted circuit parameters of the negative array by fitting the double-diode model (see Figure 2) in Hejri¹³ to the MPP data with a 3-day measurement window over a span of 20 years (from 1994 to 2014). The positive array also shows a very similar result, therefore not included here. The maximum photocurrent (J_{PH}) fluctuates possibly because of the accumulation of dust/snow or the recalibration of the pyranometer during site maintenance. However, it is expected that this fluctuation in J_{PH} does not disturb the extraction of other parameters because the double-diode model assumes voltage-independent J_{PH} , and therefore, the fluctuation will just shift the IV in Figure 4 but not change the underlying IV characteristics (shape). Remarkably, it appears that all the circuit parameters in Figure 7 were degrading (eg, shunt resistance (R_{SH}) reduces, and series

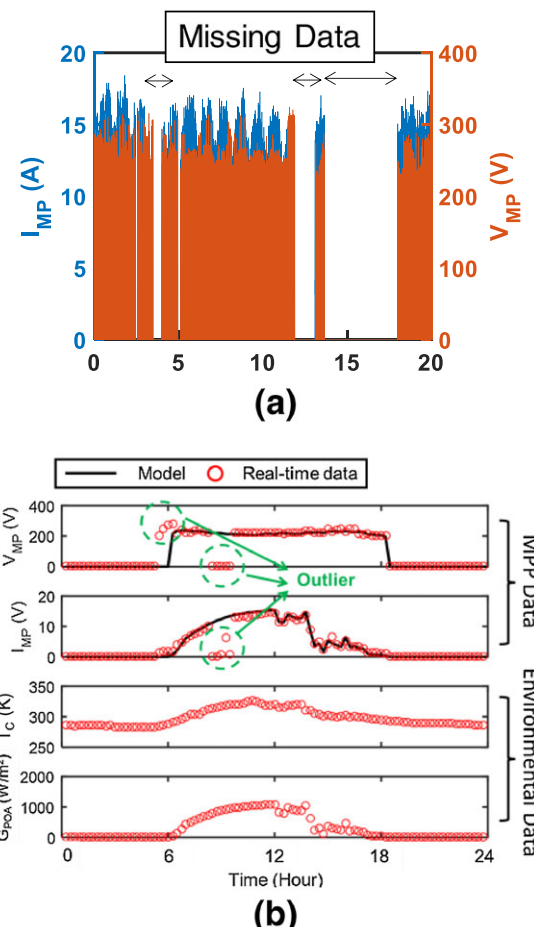


FIGURE 6 A, Twenty-year data of I_{MP} and V_{MP} of the negative monopole. B, One-day data exhibit the existence of corrupted outlier points [Colour figure can be viewed at wileyonlinelibrary.com]

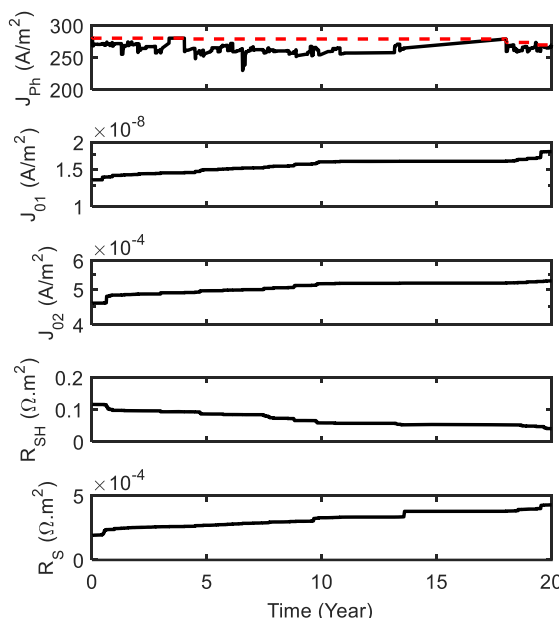


FIGURE 7 The extracted circuit parameters at the standard test condition of the double-diode model for the negative monopole as a function of time. J_{PH} is corrected so that it monotonically decreases with time (red dashed line) [Colour figure can be viewed at wileyonlinelibrary.com]

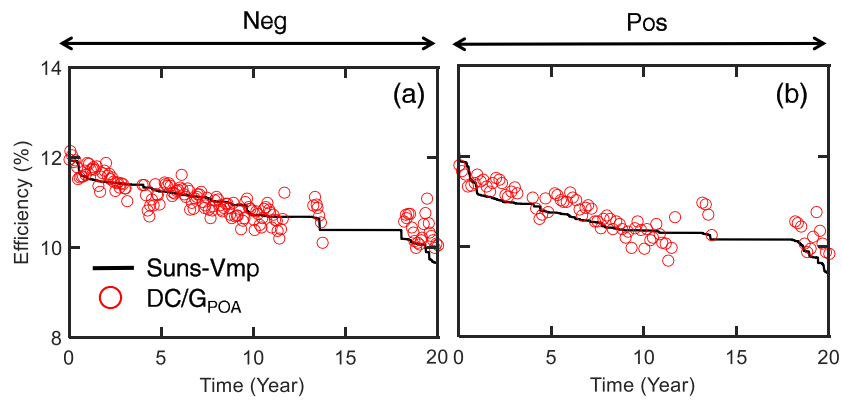


FIGURE 8 Temporal standard test condition efficiencies calculated by the Suns-Vmp and DC/G_{POA} methods for the arrays with (A) negative and (B) positive monopoles, respectively [Colour figure can be viewed at wileyonlinelibrary.com]

resistance (R_S) increases). To quantify the degradation rate, we calculate the efficiency at STC at each time step; see Figure 8.

3.2.1 | Validation 1: comparison to DC/G_{POA} method

Remarkably, the extracted STC efficiency by the Suns-Vmp method compares well with that of the conventional DC/G_{POA} method,⁶ showing both the negative and positive arrays near their warranty lifetime (80% of initial efficiency). However, the result obtained from the DC/G_{POA} method shows greater fluctuation than the Suns-Vmp method because of (1) the empirical approaches to filtering outliers and (2) linear temperature correction of real-time output power to STC by a constant temperature coefficient (which changes over time). Because the Suns-Vmp method uses a physics-based equivalent circuit for outlier filtering and temperature correction, the fluctuation is substantially reduced. Because soiling loss is recoverable, the extracted J_{PH} sometimes increases as a function of time; see the black solid line in the top plot of Figure 7. In this analysis, we only consider degradation mechanisms that causes irreversible J_{PH} losses (eg, yellowing and EVA delamination). Therefore, we correct J_{PH} such that it monotonically decreases with time; see the red dashed line in Figure 7.

3.2.2 | Validation 2: outdoor IV measurement

To further validate the Suns-Vmp method, we benchmark the results against those characterized by the periodic outdoor IV measurements throughout 20 years. Figure 9 shows the comparison between real-time (not STC) PV performance metrics calculated by circuit parameters deduced by the Suns-Vmp method and direct outdoor IV measurements. Indeed, we find excellent agreement (less than 4% mean absolute percentage error) between these 2 methods, which corroborates the accuracy of the Suns-Vmp method.

3.2.3 | Validation 3: parameter degradation rates

We also benchmark the rates of change of the performance metrics estimated from the Suns-Vmp method against the outdoor IV data from Jordan et al.³⁷ As shown in Figure 10 (top), the results are again in good agreement. The error bars are calculated within 95% confidence interval. The degradation rate of the efficiencies for both the negative and positive arrays are around 0.7%/year. It is noteworthy that the efficiency erosion can be primarily attributed to the reduction in fill factor (-0.6 to -0.4%/year), while V_{oc} and I_{sc} degradation are insignificant.

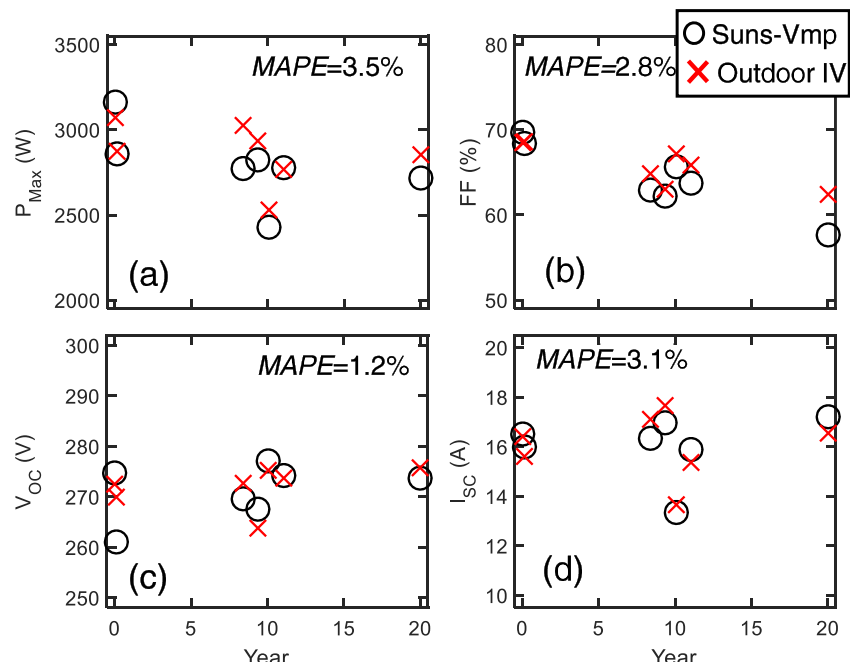


FIGURE 9 Comparison of performance metric generated by the Suns-Vmp method and outdoor array IV measurements for the negative monopole. The mean absolute percentage errors are also labeled in each plot [Colour figure can be viewed at wileyonlinelibrary.com]

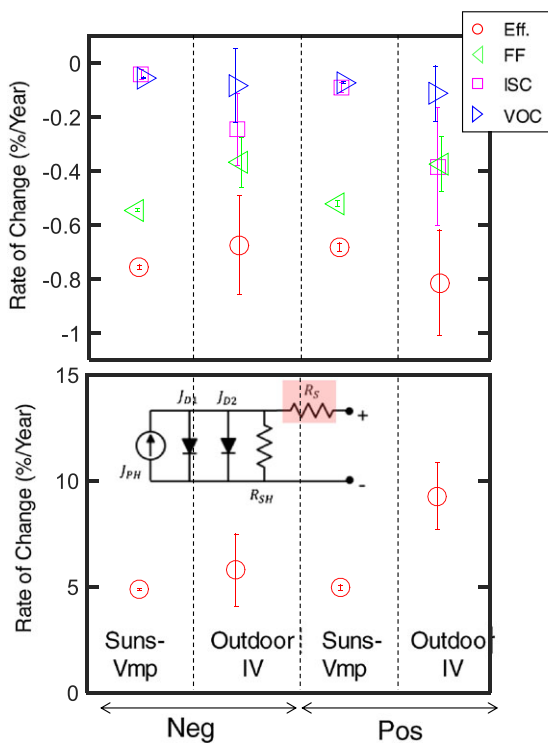


FIGURE 10 Rate of change of the performance metrics (top) and series resistance R_S (bottom) of the analyzed photovoltaic systems via the Suns-Vmp method and outdoor IV measurements [Colour figure can be viewed at wileyonlinelibrary.com]

We attribute this FF degradation to the increased series resistance, which erodes fill factor without substantially affecting Voc and Isc. Both the Suns-Vmp and outdoor IV measurement reveal the rapid increment of series resistance at the rate of 5% to 10%/year as shown in Figure 10 (bottom), which confirms our conjecture of series resistance-induced efficiency degradation.

3.2.4 | Validation 4: onsite inspection

Next, we will deconvolve and quantify the power losses ascribed to each circuit parameter to identify the predominant physical degradation pathways. As shown in Figure 11A, we deconvolve the power

losses associated with each parameter for the negative monopole. There are 3 key observations:

- At the end of 20 years, Figure 11A elucidates that the increased series resistance is the dominant contributor to efficiency reduction for the negative monopole. Remarkably, the on-site infrared image in Figure 11B exhibits localized hot spots caused by solder bond failure, in accord with our deconvolution analysis of increased series resistance. It is generally known that solder bond failure is caused by the differential thermal expansion between the solder joints and surrounding materials during repeated thermal cycling.^{38,39} Therefore, solder bonds fail (crack) in a stepwise fashion.⁴⁰ Indeed, we find the signature of this stepwise increase in the series resistance in the Suns-Vmp analysis; see Figure 11A.
- Discoloration of the encapsulants is expected because of the relatively high ultraviolet light concentration at Denver (altitude of ~1800 m).⁴¹ Indeed, a photograph of the solar modules in the field shows that the majority of the solar cells suffers from discoloration; see Figure 11C. Meanwhile, notwithstanding the J_{PH} fluctuation shown in Figure 7, our deconvolution results also manifests a symmetric decrease of J_{PH} and ascribes a significant amount of power loss (~4%) to J_{PH} reduction, an indicator of discoloration. This agreement again confirms the degradation pathways diagnosed by the Suns-Vmp method. It is noteworthy that the photocurrent reduction because of discoloration has occurred within the first year of installation. Another study has also found early advent of discoloration, ie, discoloration has been seen in 50% of the solar module less than 5 years old.⁴²
- The operating voltage of the modules is only around 200 V; therefore, the efficiency degradation because of PID is expected to be insignificant.⁴³ Indeed, our result confirms this conjecture by showing that only ~3% power loss is because of shunting (R_{SH}) and increased recombination currents (J_{02}), both of which are effective indicators for PID.^{44,45}

As demonstrated here, the Suns-Vmp method allows us to quantitatively and qualitatively diagnose the pathology of degraded solar modules exposed in the field by analyzing and interpreting the time

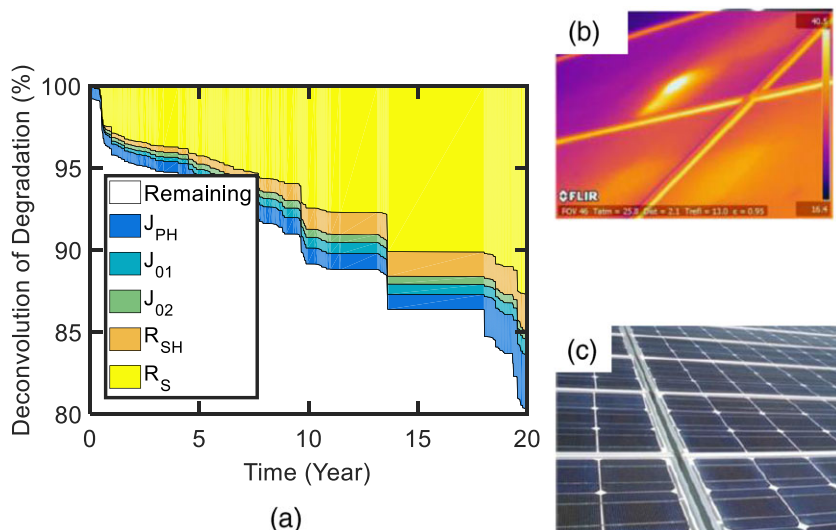


FIGURE 11 A, Temporal degradation deconvolution with respect to circuit parameters for the negative monopole. B, IR image shows a hot spot caused by solder bond failure. C, Picture shows that most cells suffer from discolouration in the center. *(B) and (C) are obtained from Jordan et al³⁷ (©IEEE 2015, reprinted with permission) [Colour figure can be viewed at wileyonlinelibrary.com]

signature of individual circuit parameters. All the results have been validated by both outdoor IV measurement and on-site characterization.

4 | DISCUSSION

In the previous section, we have applied the Suns-Vmp method to an NREL test facility and demonstrated its capability of analyzing the degradation of solar modules in real time. Next, we discuss the potential use of the time-dependent parameters obtained through the analysis and limitations of the approach.

4.1 | Geography-specific and technology-specific reliability-aware design

The underlying physical degradation mechanisms of PV are strongly contingent on local meteorological factors and different technologies, eg, solar modules exposed in humid regions are more susceptible to contact corrosion,⁴⁶ and monolithic thin-film solar modules are vulnerable to partial shading degradation.³² Similarly, modules more likely to suffer from PID should adopt Corning® Willow™ Glass to impede ion migration.⁴⁷ Therefore, ideally, module design ought to be geography and technology dependent. However, solar modules are often overdesigned for reliability (perhaps at a considerable cost) so that they can survive a broad range of weather conditions. This is because of the lack of comprehensive understanding of local degradation. The Suns-Vmp method offers an opportunity to effectively diagnose the degradation pathways of fielded solar modules of different technologies across the entire world. The results can be ultimately collected in a global database, allowing manufacturers to design and produce the next-generation reliable-aware PV module with maximized durability.

4.2 | More accurate long-term reliability prediction

Accurate prediction of long-term energy production is crucial to evaluating the bankability of investing solar farms. Various degradation pathways depend nonlinearly on stress time and local stress factors (irradiance, voltage, moisture, temperature). Therefore, it is difficult to predict future energy yields based on empirical linear degradation models.² In this regard, the Suns-Vmp method can facilitate accurate reliability prediction. Recently, several physics-based degradation models have been developed that can directly map various PV degradation modes (eg, corrosion, PID, yellowing) to the temporal behavior of circuit parameters.^{48,49} The extracted circuit parameters by the Suns-Vmp method can be used to calibrate these degradation models (eg, moisture diffusion coefficient for corrosion). Integrated with the weather forecast, the calibrated degradation models will predict the lifespan of solar modules. Alternatively, the time-dependent circuit parameters can train machine learning algorithms; the trained machine learning algorithms can predict PV lifetime. The validity of these predictive approaches, however, remains an interesting open question and requires more rigorous research efforts.

4.3 | Guidance for collecting field data

The Suns-Vmp method highlights the importance of physics-based modeling in creating databases. For example, we have seen that fitting of the pristine module characteristics requires temperature-dependent and illumination-dependent IV measurement to ensure a robust and unique initial guess. Second, we have noted that weather data may be corrupted or missing. Thus, it is important for PV databases to contain complementary information from multiple sources.⁵⁰ Finally, circuit model parameters offer an important recipe for improving data compression and computational efficiency; the model parameters can diagnose the module by only deciphering the stored Vmp-Imp information (a byproduct data of normal operation at MPP) for the entire duration. This eliminates the need for deliberate measurement of massive IV data¹¹ and time-consuming trip to collect field data.⁴²

4.4 | Intrastring variability

Process-induced variability can lead to performance variation in the cell, module, or array levels,^{26,51,52} especially for the thin-film PV where binning is not possible. Similarly, various degradation modes introduce local variability as well: for example nonuniform degradation (eg, cells adjacent to module edges are more prone to contact corrosion than those located away from the edges⁵³; solar modules close to the negative array are more susceptible to PID⁵⁴). The Suns-Vmp method uses a single equivalent circuit to analyze a string consisting of multiple modules and thus accounts for “average” circuit parameters. As a result, it is critical to investigate how performance variability can potentially affect the accuracy of the Suns-Vmp method. Therefore, we have tested the Suns-Vmp method under various scenarios of performance variability, and the results are listed in Sec. D of the SI. Remarkably, our findings highlight that the circuit parameters extracted by the Suns-Vmp method are still valid to interpret PV degradation with moderate nonuniformity. Affected by severe nonuniformity, however, the Suns-Vmp method may not be able to identify the primary circuit parameters contributing to power losses. For these cases, it will be important to represent the string by a few equivalent circuit models. Despite the increase in the parameter number, the following considerations are expected to simplify the calibration process: (1) availability of time-zero information of each module, (2) the large amount of data available within the measurement window, and (3) several degradation modes (eg, yellowing) are expected to affect all the modules uniformly, while others (eg, PID) are more pronounced in a few solar modules with high voltage bias at the end of a string. The ability to account for nonuniform degradation will be an important direction of future research on this topic.

4.5 | Analyzing thin-film modules by the Suns-Vmp method

In this paper, we have focused on the degradation of c-Si modules. Thin-film solar modules degrade differently compared to silicon modules. For example, thin-film solar modules are more susceptible to intrinsic material degradation⁵⁵ and partial shading degradation.³² With 2 modifications, the Suns-Vmp method can be extended to study

the reliability of thin-film solar modules. First, because the conventional single-diode and double-diode models cannot capture the physics of thin-film solar cells (eg, voltage-dependent photocurrent), one needs to adopt new circuit models. Sun et al,²⁴ Sun et al,²⁵ Sun et al,⁵⁶ and Crandall⁵⁷ developed a set of physics-based circuit models for a-Si, perovskite, CIGS, and CdTe solar cells. These models also contain physical parameters pertaining to degradation pathways unique to these thin-film technologies, eg, s_f and s_b in Sun et al²⁵ can describe the interface degradation in a perovskite solar cell.⁵⁸ Hence, these models enable diagnosis of these technology-specific degradation processes. Second, some thin-film solar modules exhibit efficiency metastability (eg, light soaking⁵⁹), which needs special treatments in preprocessing the field data. It has been found that CdTe modules require >5000 hours of light soaking to stabilize long-term performance⁶⁰; thereby, to exclude the effect of metastability, only stabilized field data after sufficient preconditioning should be used in the Suns-Vmp method. This precondition time can also vary as a function of technology, temperature, and voltage bias, all of which must be accounted for as well.

5 | CONCLUSIONS

To summarize, we have presented a novel method, ie, the Suns-Vmp method, for analyzing the PV degradation:

1. The Suns-Vmp method enables monitoring and diagnosis of PV reliability in real time by systemically and physically mining the time series MPP data. The method can extract physically defined circuit parameters by fitting IVs consisting of the varying MPP data over a measurement window. The extracted circuit parameters can be used to estimate the STC efficiency, quantitatively deconvolve PV degradation pathways, and identify the dominant degradation pathways. The MATLAB code for the Suns-Vmp method is also available online.²³
2. We have demonstrated the Suns-Vmp method by analyzing MPP data from an NREL test facility, where physics-based circuit parameters and efficiencies of the solar modules have been extracted as a function of time. Independent outdoor IV measurements have systemically validated our results. Our analysis suggests that the PV system degrades at a rate of 0.7%/year, primarily because of reduced short-circuit current and increased series resistance most likely caused by discoloration and weakened solder bond, respectively. The on-site optical photograph and IR image indeed substantiate our interpretation of the physical degradation pathways, ie, discoloration and solder bond failure.
3. The analysis of deconvolving the underlying degradation pathways by the Suns-Vmp method can deepen the current understanding of technology-dependent and geographic-dependent degradation, and inspire more robust environment-specific designs for the next-generation reliability-aware solar modules. The Suns-Vmp method can be used to calibrate physics-based degradation models as well as train machine learning algorithms, both of which can then predict power degradation of PV and improve the evaluation of “bankability.”

ACKNOWLEDGEMENTS

This work was supported by the US-India Partnership to Advance Clean Energy-Research (PACE-R) for the Solar Energy Research Institute for India and the United States (SERIUS) and the DEEDS program by the National Science Foundation under award #1724728. The authors would like to thank Dr. Haejun Chung, Reza Asadpour, and Dr. Mohammad Ryyan Khan for helpful discussion, Dr. Chris Deline and Dr. Dirck Jordan for providing IV measurement, as well as Prof. Mark S. Lundstrom and Prof. Peter Bermel for kind guidance.

ORCID

Xingshu Sun  <http://orcid.org/0000-0002-2511-0076>

Raghu Vamsi Krishna Chavali  <http://orcid.org/0000-0002-8917-2639>

REFERENCES

1. Jordan DC, Silverman TJ, Sekulic B, Kurtz SR. PV degradation curves: Non-linearities and failure modes. *Prog Photovoltaics Res Appl*. 2016;15, no February 2013:659-676.
2. Jordan DC, Kurtz SR, VanSant K, Newmiller J. Compendium of photovoltaic degradation rates. *Prog Photovoltaics Res Appl*. 2016; 24(7):978-989.
3. Ndiaye A, Charki A, Kobi A, Kébé CMF, Ndiaye PA, Sambou V. Degradations of silicon photovoltaic modules: A literature review. *Sol Energy*. 2013;96:140-151.
4. Belluardo G, Ingenhoven P, Sparber W, Wagner J, Weihs P, Moser D. Novel method for the improvement in the evaluation of outdoor performance loss rate in different PV technologies and comparison with two other methods. *Sol Energy*. 2015;117:139-152.
5. Jordan DC, Kurtz SR. The dark horse of evaluating long-term field performance—data filtering. *IEEE J. Photovoltaics*. 2014;4(1):317-323.
6. Jordan DC, Kurtz S. 2012 PV degradation risk, in the World Renewable Energy Forum, 2012.
7. Haeberlin H, Beutler C. Normalized representation of energy and power for analysis of performance and on-line error detection in PV-systems, in European Photovoltaic Solar Energy Conference and Exhibition, 17th, 1995.
8. Jennings C. PV module performance at PG&E, in *Conference Record of the Twentieth IEEE Photovoltaic Specialists Conference*, 1988;2: 1225-1229.
9. French RH, Podgornik R, Peshek TJ, et al. Degradation science: Mesoscopic evolution and temporal analytics of photovoltaic energy materials. *Curr Opin Solid State Mater Sci*. 2015;19(4):212-226.
10. Peshek TJ, Fada JS, Hu Y, et al. Insights into metastability of photovoltaic materials at the mesoscale through massive I–V analytics. *J Vac Sci Technol B, Nanotechnol Microelectron Mater Process Meas Phenom*. 2016;34(5):50801.
11. Hu Y, Gunapati VY, Zhao P, et al. A nonrelational data warehouse for the analysis of field and laboratory data from multiple heterogeneous photovoltaic test sites. *IEEE J. Photovoltaics*. 2017;7(1):230-236.
12. Wu Y-K, Chen C-R, Abdul Rahman H. A novel hybrid model for short-term forecasting in PV power generation. *Int J Photoenergy*. 2014;2014:1-9.
13. Hejri M, Mokhtari H, Azizian MR, Ghandhari M, Soder L. On the parameter extraction of a five-parameter double-diode model of photovoltaic cells and modules. *IEEE J. Photovoltaics*. 2014;4(3):915-923.
14. Jordan DC, Deline C, Johnston S, et al. Silicon heterojunction system field performance. *IEEE J. Photovoltaics*. 2018;8(1):177-182.
15. J. Sutterlueti, S. Ransome, J. Stein, and J. Scholz, Improved PV performance modelling by combining the PV_LIB toolbox with the Loss

- Factors Model (LFM), in 2015 IEEE 42nd Photovoltaic Specialist Conference (PVSC), 2015, pp. 1–6.
16. Ransome S, Sutterlueti J. Determining the causes and rates of PV degradation using the Loss Factors Model (LFM) with high quality IV measurements, in PV Performance and Monitoring Workshop, 2016.
 17. Trupke T, Pink E, Bardos RA, Abbott MD. Spatially resolved series resistance of silicon solar cells obtained from luminescence imaging. *Appl Phys Lett.* 2007;90(9):93506.
 18. Peike C, Hoffmann S, Hülsmann P, et al. Origin of damp-heat induced cell degradation. *Sol. Energy Mater. Sol. Cells.* 2013;116:49–54.
 19. Luo W, Khoo YS, Hacke P, et al. Potential-induced degradation in photovoltaic modules: A critical review. *Energ Environ Sci.* 2017;10(1): 43–68.
 20. Kerr MJ, Cuevas A, Sinton RA. Generalized analysis of quasi-steady-state and transient decay open circuit voltage measurements. *J Appl Phys.* 2002;91(1):399.
 21. Chavali RVK, Li JV, Battaglia C, De Wolf S, Gray JL, Alam MA. A generalized theory explains the anomalous suns-VOC response of Si heterojunction solar cells. *IEEE J. Photovoltaics.* 2017;7(1):169–176.
 22. Chavali RVK, De Wolf S, Alam MA. Device physics underlying silicon heterojunction and passivating-contact solar cells: A topical review. *Prog Photovoltaics Res Appl.* 2018;26(4):241–260.
 23. Sun X, Chavali RVK, Alam MA. Suns-Vmp method. 2018. <https://nanohub.org/resources/28580>
 24. Sun X, Silverman T, Garris R, Deline C, Alam MA. An illumination- and temperature-dependent analytical model for copper indium gallium diselenide (CIGS) solar cells. *IEEE J Photovoltaics.* 2016;1:1–10.
 25. Sun X, Asadpour R, Nie W, Mohite AD, Alam MA. A physics-based analytical model for perovskite solar cells. *IEEE J Photovoltaics.* 2015;5(5):1389–1394.
 26. Chavali RVK, Johlin EC, Gray JL, Buonassisi T, Alam MA. A framework for process-to-module modeling of a-Si/c-Si (HIT) heterojunction solar cells to investigate the cell-to-module efficiency gap. *IEEE J. Photovoltaics.* 2016;6(4):1–13.
 27. Dongaonkar S, Servaites JD, Ford GM, et al. Universality of non-Ohmic shunt leakage in thin-film solar cells. *J Appl Phys.* 2010;108(12): 124509.
 28. Lee K. Improving the PV module single-diode model accuracy with temperature dependence of the series resistance, in IEEE 44th Photovoltaic Specialist Conference (PVSC), 2017.
 29. Chavali RVK, Moore JE, Wang X, Alam MA, Lundstrom MS, Gray JL. The frozen potential approach to separate the photocurrent and diode injection current in solar cells. *IEEE J. Photovoltaics.* 2015;5(3):865–873.
 30. Siemens Solar Panels Installation Guide. [Online]. Available: http://iodlabs.ucsd.edu/dja/codered/Engineering/procedures/solarPower/siemens_solar_panels.pdf.
 31. Matlab2016a. The MathWorks Inc, Natick, MA, 2016.
 32. Silverman TJ, Deceglie MG, Sun X, et al. Thermal and electrical effects of partial shade in monolithic thin-film photovoltaic modules. *IEEE J. Photovoltaics.* 2015;5(6):1742–1747.
 33. Hacke P, Spataru S, Johnston S, et al. Elucidating PID degradation mechanisms and in situ dark I–V monitoring for modeling degradation rate in CdTe thin-film modules. *IEEE J. Photovoltaics.* 2016;6(6): 1635–1640.
 34. Hacke P, Spataru S, Terwilliger K, et al. Accelerated testing and modeling of potential-induced degradation as a function of temperature and relative humidity. *IEEE J. Photovoltaics.* 2015;5(6):1549–1553.
 35. PVDAQ (PV Data Acquisition). [Online]. Available: <http://developer.nrel.gov/docs/solar/pvdaq-v3/>.
 36. Faiman D. Assessing the outdoor operating temperature of photovoltaic modules. *Prog Photovoltaics Res Appl.* 2008;16(4):307–315.
 37. Jordan DC, Sekulic B, Marion B, Kurtz SR. Performance and aging of a 20-year-old silicon PV system. *IEEE J. Photovoltaics.* 2015;5(3): 744–751.
 38. Itoh U, Yoshida M, Tokuhisa H, Takeuchi K, Takemura Y. Solder joint failure modes in the conventional crystalline si module. *Energy Procedia.* 2014;55(3):464–468.
 39. Shen Y-L. Numerical study of solder bond failure in photovoltaic modules. *Procedia Eng.* 2016;139:93–100.
 40. Vasudevan V, Fan X. An acceleration model for lead-free (SAC) solder joint reliability under thermal cycling, in 2008 58th Electronic Components and Technology Conference. 2008;139–145.
 41. Kempe MD. Ultraviolet light test and evaluation methods for encapsulants of photovoltaic modules. *Sol Energy Mater Sol Cells.* 2010;94(2):246–253.
 42. Chattopadhyay S, Dubey R, Kuthanazhi V, et al. Visual degradation in field-aged crystalline silicon PV modules in India and correlation with electrical degradation. *IEEE J. Photovoltaics.* 2014;4(6):1470–1476.
 43. Hattendorf J, Löw R, Gnehr W-M, Wulff L, Koekten MC, Koschnicharov D, Blauermel A, Esquivel JA. Potential induced degradation in monocrystalline silicon based modules: An acceleration model, in 27th EU PVSEC. 2012;3405–3410.
 44. Lausch D, Naumann V, Breitenstein O, et al. Potential-induced degradation (PID): Introduction of a novel test approach and explanation of increased depletion region recombination. *IEEE J. Photovoltaics.* 2014;4(3):834–840.
 45. Naumann V, Lausch D, Hänel A, et al. Explanation of potential-induced degradation of the shunting type by Na decoration of stacking faults in Si solar cells. *Sol Energy Mater Sol Cells.* 2014;120, no PART A:383–389.
 46. All-India India Survey of Photovoltaic Module Degradation: 2013. [Online]. Available: http://www.ncpre.iitb.ac.in/uploads/Chendamangalam_Final_Report_e-copy_upload.pdf.
 47. Oh J, TamizhMani G, Bowden S, Garner S. Surface disruption method with flexible glass to prevent potential-induced degradation of the shunting type in PV modules. *IEEE J. Photovoltaics.* 2016;2156:1–6.
 48. Asadpour R, Chavali RVK, Alam MA. Physics-based computational modeling of moisture ingress in solar modules: Location-specific corrosion and delamination, in 2016 IEEE 43rd Photovoltaic Specialists Conference (PVSC). 2016;0840–0843.
 49. Bermel P, Asadpour R, Zhou C, Alam MA. A modeling framework for potential induced degradation in PV modules, in SPIE, 2015;95630C.
 50. Zhao B, Sun X, Alam MA, Khan MR. Purdue University Meteorological Tool. [Online]. Available: <https://nanohub.org/resources/pumet>.
 51. Dongaonkar S, Loser S, Sheets EJ, et al. Universal statistics of parasitic shunt formation in solar cells, and its implications for cell to module efficiency gap. *Energ Environ Sci.* 2013;6(3):782.
 52. Mungan ES, Wang Y, Dongaonkar S, Ely DR, Garcia RE, Alam MA. From process to modules: End-to-end modeling of CSS-deposited CdTe solar cells. *IEEE J. Photovoltaics.* 2014;4(3):954–961.
 53. Kempe MD. Modeling of rates of moisture ingress into photovoltaic modules. *Sol Energy Mater Sol Cells.* 2006;90(16):2720–2738.
 54. Pingel S, Frank O, Winkler M, Daryan S, Geipel T, Hoehne H, Berghold J. Potential induced degradation of solar cells and panels, in 2010 35th IEEE Photovoltaic Specialists Conference, 2010;002817–002822.
 55. Ray B, Alam MA. A compact physical model for morphology induced intrinsic degradation of organic bulk heterojunction solar cell. *Appl Phys Lett.* 2011;99(3):1–4.
 56. Sun X, Raguse J, Garris R, Deline C, Silverman T, Alam MA. A physics-based compact model for CIGS and CdTe solar cells: From voltage-dependent carrier collection to light-enhanced reverse breakdown, in 2015 IEEE 42nd Photovoltaic Specialist Conference (PVSC), 2015;1–6.
 57. Crandall RS. Modeling of thin film solar cells: Uniform field approximation. *J Appl Phys.* 1983;54(12):7176–7186.
 58. Xiong J, Yang B, Cao C, et al. Interface degradation of perovskite solar cells and its modification using an annealing-free TiO₂ NPs layer. *Org Electron.* 2016;30:30–35.

59. Silverman TJ, Deceglie MG, Marion B, Kurtz SR. Performance stabilization of CdTe PV modules using bias and light. *IEEE J. Photovoltaics*. 2015;5(1):344-349.
60. Gostein M, Dunn L. Light soaking effects on PV modules: Overview and literature review, *the NREL PV Module Reliability Workshop*, 2011. [Online]. Available: https://www1.eere.energy.gov/solar/pdfs/pvmrw2011_p25_tf_dunn.pdf.

How to cite this article: Sun X, Chavali RVK, Alam MA. Real-time monitoring and diagnosis of photovoltaic system degradation only using maximum power point—the Suns-Vmp method. *Prog Photovolt Res Appl*. 2019;27:55–66. <https://doi.org/10.1002/pip.3043>

SUPPORTING INFORMATION

Additional supporting information may be found online in the Supporting Information section at the end of the article.

Real-time monitoring and diagnosis of photovoltaic system degradation only using maximum power point—the Suns-Vmp method

Xingshu Sun, Raghu Vamsi Krishna Chavali, and Muhammad Ashraful Alam

Network of Photovoltaic Technology, Purdue University, West Lafayette, IN, 47907, USA

Supplementary Information

A. Summary of On- and Off-line Techniques

Table S1 summarizes typical on- and off-line techniques to characterize degradation pathways of solar modules.

Table. S1 A detailed summary of various on/off-line methods			
Name	Procedure	Outcome	Limitation
Online method			
<i>DC/G_{POA}</i> [1]	The ratio of temperature-corrected DC power over the plane-of-array irradiance	Time-series STC efficiency and degradation rate	Can not identify the primary degradation pathways
Performance Ratio (PR) [2]	$PR = \frac{Y_G}{Y_R}$ where Y_G and Y_R are respectively the generated output energy and the reference output energy (i.e., calculated by nameplate ratings)		
Photovoltaics for Utility Scale Applications (PVUSA) [3]	Use linear regression to translate real-time power to values under the standard test condition (STC) as a function of irradiance, ambient temperature, and wind speed		
Machine Learning [4]–[7]	Apply classification and regression algorithms to analyze field data	Short- and long-term energy forecast, identify anomalous IV	Data-intensive, lack of physical interpretation
Off-line method			
IV Measurement [8], [9]	Apply circuit models to analyze intermittent IV measurements	Calculate STC efficiencies and degradation rates, identify degradation pathways via circuit parameters	Interrupt the operation of PV systems
Advanced Imaging Techniques [10]–[12]	Measure optical/thermal signals of solar modules (e.g., luminescence of a biased solar cell for electroluminescence)	Map position-resolved defects (e.g., shunt, cracking) and parameters (e.g., series resistance)	
Material Characterization [13]	Measure the microscopic structure and material composition of a solar cell	Investigate the fundamental physics of PV degradation processes	
Suns-Voc [8], [14], [15]	Measure open-circuit voltage under different illumination intensities	Calculate series resistance, bias-dependent photocarrier lifetime, and heterojunction-related degradation	

B. Preprocessing of the Environmental Data

The Suns-Vmp method requires environment data, i.e., cell temperature and irradiance. The environment data is used as an input to the equivalent circuit to fit the reconstructed MPP IV. The raw environmental data sometimes contain corrupted or inconsistent entries. Hence, it is vital to preprocess the raw data to correct for these variations such that the circuit parameters

extracted are accurate and robust. Below, we discuss in detail the procedure used in this paper to preprocess the environmental data.

Cell Temperature. Module temperature is typically measured by the thermal sensors attached to the back side of solar modules. It has been shown that the actual cell temperature is usually higher than the measured back-side module temperature [16]. Ref. [16] has developed an empirical equation to predict cell temperature (T_C) based on illumination intensity (G_{POA}) and back-side module temperature (T_M). We have employed this empirical equation in the Suns-Vmp method to calculate T_C .

Irradiance Data. In addition to thermal information, we also need illumination data to perform the Suns-Vmp method. The on-site illumination data is typically measured by a pyranometer orientated and tilted with the same angle as the solar modules to collect the identical plane-of-array irradiance G_{POA} . However, directly applying the raw G_{POA} data to the Suns-Vmp method can lead to inaccuracy in extracting short-circuit current because of 1) air mass dependent spectral mismatch between the field and the standard test condition (STC), and 2) reflection loss of flat-plate solar modules. Thus, one must preprocess G_{POA} data to eliminate the above non-idealities as below:

1. **Spectral Mismatch.** The spectral profile of G_{POA} under which MPP data is generated can differ from the standard AM1.5G spectrum used for initial rating under STC. Because the extracted circuit parameters from the Suns-Vmp method are eventually corrected to their STC values, the spectral mismatch between real-time field irradiance and STC can contaminate the fitting results, especially the short-circuit current. Fortunately, the Sandia PV Array Performance Model (SAPM) has developed a polynomial equation to empirically describe the spectral content of solar irradiance as a function of air mass (AM) [16]. In this paper, we use the SAPM to correct the real-time G_{POA} to its STC values, where AM is calculated by the Sandia PV modeling library [17] and the Direct Normal Incidence (DNI) is retrieved from [18] at the installation location.
2. **Reflection Loss.** Pyranometers can accept irradiance coming from a highly oblique angle of incidence (AOI) thanks to the dome-shaped glass cover, while flat-plane solar modules are susceptible to reflection loss at high AOI. Consequently, one must also adjust G_{POA} measured by pyranometers to account for reflection loss. In this paper, given the tilt and azimuth angles of the analyzed solar modules, we utilize SAPM to correct for reflection loss of DNI.

Although meteorological information is often available from on-site weather stations, this may not be the always the case. In the absence of on-site meteorological data, comprehensive meteorological databases, such as Refs. [18], [19] can be alternative sources for reproducing illumination and temperature information.)

C. Physics-Based Filtering Algorithm

Outlier data points due to instrumentation errors, inverter clipping, weather condition, etc., may occur in the field data [20]. For example, the Imp data point at around 9 am in Fig. S1 is inconsistent with G_{POA} ; thereby, this data point should be regarded as an outlier and discarded in the Suns-Vmp method. The inclusion of these outliers can induce significant uncertainties in

extracting circuit parameters. Therefore, it is necessary to develop a self-consistent scheme to detect and remove these outliers. Toward this goal, we have created a continuous physics-based self-filtering algorithm to eliminate outlier data points, see Fig. S2. The steps are as follows:

- 1) Fit the MPP data with non-zero POA irradiance using the equivalent circuit (MPP data with zero irradiance always yields zero current and voltage, thereby irrelevant in the fitting process). This fitting step is confined to the MPP data only within the measurement window at a single time step.
- 2) Calculate the relative error of fitting each MPP data point. If the error is greater than 50%, the corresponding data point is treated as an outlier and discarded.
- 3) Examine the number of the remaining data points after step 2. If the remaining still consists of more than 80% of the raw data points, proceed to step 4. Otherwise, the corresponding time step is considered as an outlier as a whole (i.e., remove all the data points at this time step). The Suns-Vmp method will directly move to the next time window. The entire measurement window may consist of corrupted data if temporary instrumentations malfunctions for more than a few days.
- 4) Fit the filtered MPP data by the equivalent circuit and extract the circuit parameters.
- 5) Move to next time step.

Note that our continuous self-filtering algorithm in this paper has comprehensively accounted for outliers caused by various non-idealities (e.g., cloud brightening, inverter clipping, temperature/illumination stability, pyranometer error); thus, there is no need to create individual data filters as in [20]. Moreover, the percentage thresholds in steps 2 and 3 (i.e., 50% for relative error and 80% for the number of remaining data points) are found to work well for analyzing field data, and we do not expect that a moderate adjustment of the percentage thresholds will significantly impact the outcome. Enabled by our filtering algorithm, excellent error control has been achieved, i.e., the relative error is less than 5% for both V_{mp} and I_{mp} through the entire 20-year analysis.

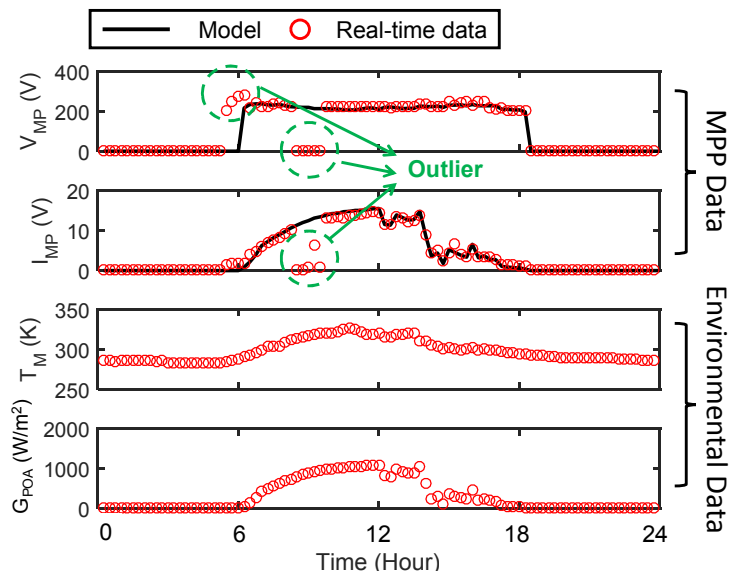
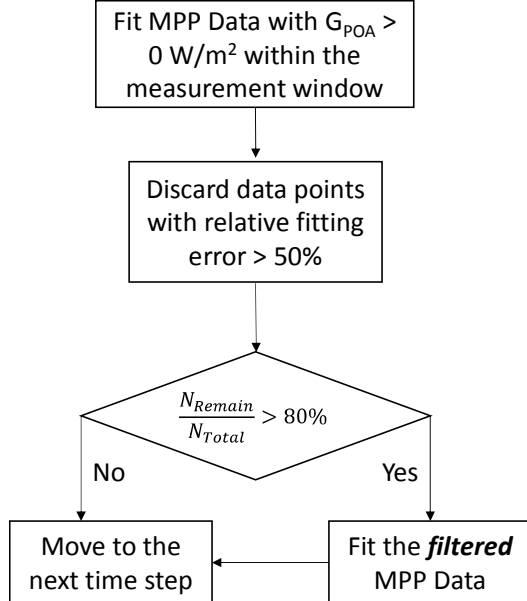


Fig. S1 Raw MPP data with outliers, fitting results of the filtered MPP data, and the environmental data of the NREL test facility on 05/16/1994.



* N_{Remain} and N_{Total} are the numbers of remaining and total data points, respectively.

Fig. S2 Flowchart of our self-filtering algorithm to identify and eliminate outlier data points.

D. Variability Test of the Suns-Vmp Method

Solar cells in a module may be subject to different external stressors and thus degrade in a non-uniform manner (e.g., cells at the end of a string suffer more from potential induced degradation (PID) due to higher voltage). Therefore, it is critical to test the Suns-Vmp method in the case of non-uniform degradation.

We have tested the Suns-Vmp method on solar modules with various scenarios of cell-to-cell variability using synthetic weather data in Fig. S3. Specifically, we have emulated four cases of variability: 1) 6 out of 36 cells degrades due to solder bond failure (R_s increases tenfold); 2) 6 out of 36 cells have encapsulant delamination (only retain 80% of initial short-circuit current); 3) 6 out of 36 cells suffer from moderate potential-induced degradation (shunt resistance decrease by one order); 4) 6 out of 36 cells suffer from sever potential-induced degradation (shunt resistance decrease by two orders). All the tests of performance variability are summarized in Figs. S4 to S7.

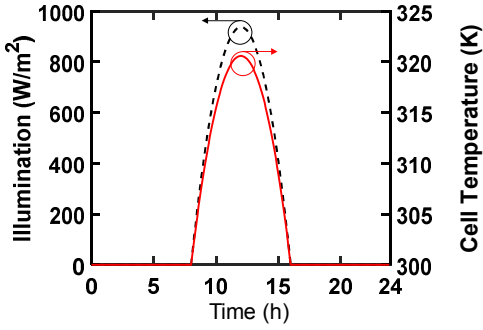
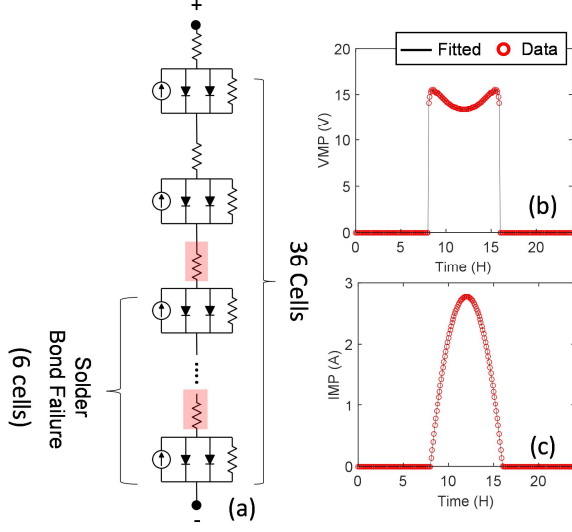


Fig. S3 Synthetic weather data containing hourly illumination and cell temperature is used to test the Suns-Vmp method.

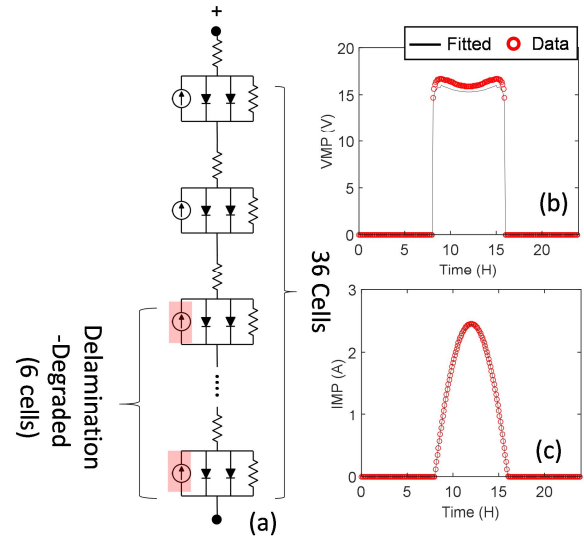
As shown in Figs. S4 – S7, the Suns-Vmp method is still capable of diagnosing the pathology of solar modules with non-uniform degradation. For example, the Suns-Vmp method has attributed efficiency degradation to increased series resistance in Fig. S4. This result, however, is not surprising since the series-connected series resistors in Fig. S4(a) can essentially be aggregated into one single resistor. Remarkably, the Suns-Vmp method is still valid even for non-uniform delamination- and PID-induced degradation where simple superposition of either short-circuit current and shunt resistance of “good” and degraded cells does not hold, see Figs. S5 and S6. The Suns-Vmp, however, cannot correctly extract the degraded circuit parameters under severe performance variability, see Fig. S7. Hence, it is recommended to utilize multiple equivalent circuits to cope with substantial performance variability.



(d) Extracted parameter by the Suns-Vmp method

	Default (30 cells)	Degraded (6 cells)	Extraction
282 A/m ²	282 A/m ²	282 A/m ²	
1.3×10^{-8} A/m ²	1.3×10^{-8} A/m ²	1.3×10^{-8} A/m ²	
4.6×10^{-4} A/m ²	4.6×10^{-4} A/m ²	4.6×10^{-4} A/m ²	
0.12 Ω.m ²	0.12 Ω.m ²	0.12 Ω.m ²	
1.7×10^{-4} Ω.m ²	1.7×10^{-3} Ω.m²	4.2×10^{-4} Ω.m²	

Fig. S4 (a) A schematic of the simulated 36-cell solar module including 6 cells degraded due to solder bond failure. The degraded circuit elements are also highlighted. (b,c) Vmp and Imp of the solar panel using the synthetic weather data in Fig. A1. Circles are simulated data and solid lines are fitting data using the Suns-Vmp method. (d) Table summarizes input parameters (both default and degraded) and extracted parameter set using the Suns-Vmp method (affected parameters are in bold).



(d) Extracted parameter by the Suns-Vmp method

	Default (30 cells)	Degraded (6 cells)	Extraction
282 A/m ²	282 A/m ²	225 A/m²	244 A/m²
1.3×10^{-8} A/m ²			
4.6×10^{-4} A/m ²			
0.12 Ω.m ²	0.12 Ω.m ²	0.12 Ω.m ²	0.12 Ω.m ²
1.7×10^{-4} Ω.m ²			

Fig. S5 (a) A schematic of the simulated 36-cell solar module including 6 cells degraded due to delamination. The degraded circuit elements are also highlighted. (b,c) Vmp and Imp of the solar panel using the synthetic weather data in Fig. A1. Circles are simulated data and solid lines are fitting data using the Suns-Vmp method. (d) Table summarizes input parameters (both default and degraded) and extracted parameter set using the Suns-Vmp method (affected parameters are in bold).

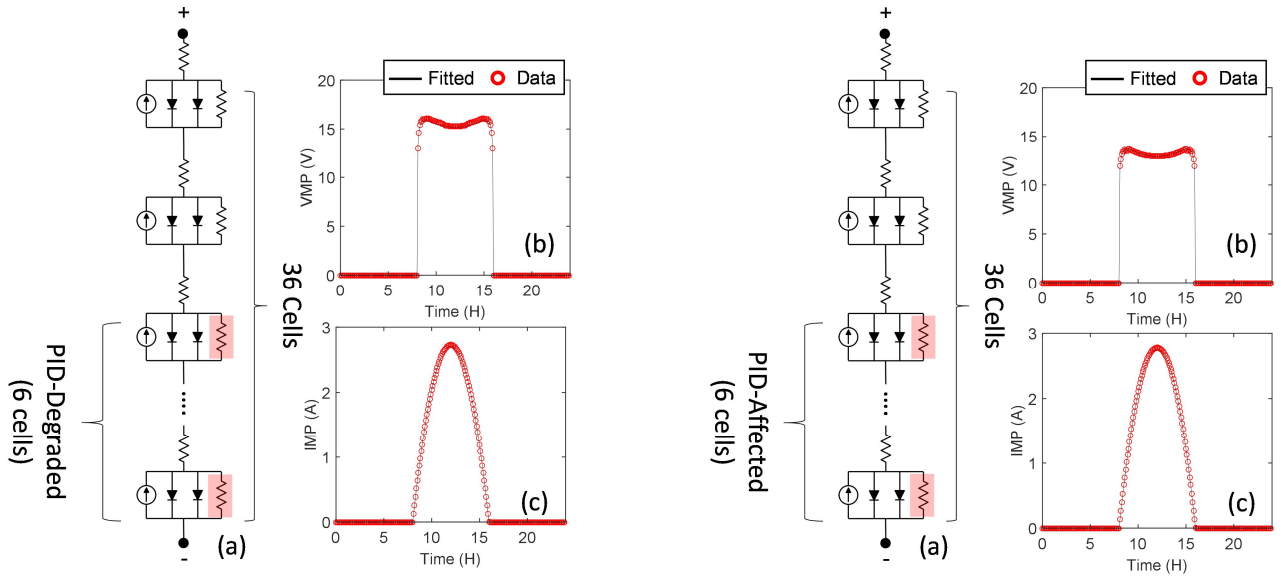


Fig. S6 (a) A schematic of the simulated 36-cell solar module including 6 cells degraded due to *moderate* potential induced degradation. The degraded circuit elements are also highlighted. (b,c) V_{mp} and I_{mp} of the solar panel using the synthetic weather data in Fig. A1. Circles are simulated data and solid lines are fitting data using the Suns- V_{mp} method. (d) Table summarizes input parameters (both default and degraded) and extracted parameter set using the Suns- V_{mp} method (affected parameters are in bold).

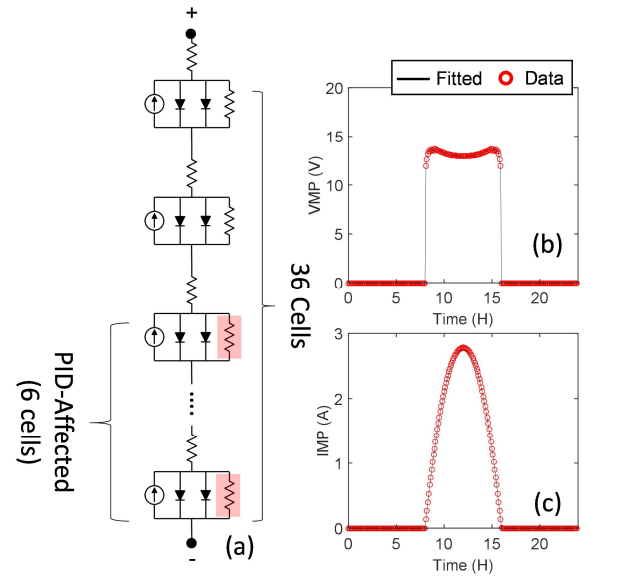


Fig. S7 (a) A schematic of the simulated 36-cell solar module including 6 cells degraded due to *severe* potential induced degradation. The degraded circuit elements are also highlighted. (b,c) V_{mp} and I_{mp} of the solar panel using the synthetic weather data in Fig. A1. Circles are simulated data and solid lines are fitting data using the Suns- V_{mp} method. (d) Table summarizes input parameters (both default and degraded) and extracted parameter set using the Suns- V_{mp} method (affected parameters are in bold).

E. Equations of the Five Parameter Model for Si Solar Modules

Here, we will present the analytical formulation of the double-diode model [21] used in this paper (see Fig. 2 in the main text) and the temperature- and illumination-dependencies of each parameter in Table S2. Also, the detailed descriptions and initial STC values for Siemens M55 [22] of each circuit parameter are listed in Table A2. Note that $G_{STC} = 1000 \text{ W/m}^2$ and $T_{STC} = 25^\circ\text{C}$ in Table S3.

Table S2. The equations of the five-parameter model

Analytical equations for I-V characteristics	
$J_{D1} = J_{01} \left(e^{\frac{q(V-JR_S)}{kT}} - 1 \right)$	(A.1)
$J_{D2} = J_{01} \left(e^{\frac{q(V-JR_S)}{2kT}} - 1 \right)$	(A.2)
$J_{Shunt} = \frac{(V - JR_S)}{R_{Shunt}}$	(A.3)
$J = J_{PH} + J_{D1} + J_{D2} + J_{Shunt}$	(A.4)
Illumination and temperature dependencies of the parameters	
J_{PH}	$J_{PH} = \frac{G}{G_{STC}} \times J_{PH,STC} \times (1 + \beta \times (T - T_{STC}))$ (A.5)
J_{01}	$J_{01} = J_{01,STC} \times \left(\frac{T}{T_{STC}} \right)^3 \times \exp\left(\frac{1}{k} \left(\frac{E_{G,STC}}{T_{STC}} - \frac{E_G}{T} \right)\right)$ (A.6)
J_{02}	$J_{02} = J_{02,STC} \times \left(\frac{T}{T_{STC}} \right)^{2.5} \times \exp\left(\frac{2}{k} \left(\frac{E_{G,STC}}{T_{STC}} - \frac{E_G}{T} \right)\right)$ (A.7)
R_{Shunt}	$R_{Shunt} = R_{Shunt,STC} \times \frac{G}{G_{STC}}$ (A.8)
E_G	$E_G = E_{G,STC} + \alpha(T - T_{STC})$ (A.9)

Table S3. Parameter description and their initial STC values for Siemens M55 [22]

$J_{SC,STC}$	Short-circuit current	282 A/m ²
$J_{01,STC}$	Diode recombination current with an ideality factor of 1	1.3×10^{-8} A/m ²
$J_{02,STC}$	Diode recombination current with an ideality factor of 2	4.6×10^{-4} A/m ²
$R_{Sh,STC}$	Shunt resistance	0.12 Ω.m ²
R_S	Series resistance	1.7×10^{-4} Ω.m ²
β	Temperature coefficient of short-circuit current	0.49 %/K
E_G	Bandgap of Si absorber	1.12 eV
α	Temperature coefficient of Si bandgap	-6×10^{-4} eV/K

References:

- [1] Jordan DC, Kurtz S. 2012 PV degradation risk, in the World Renewable Energy Forum, 2012.
- [2] Haeberlin H, Beutler C. Normalized Representation of Energy and Power for Analysis of Performance and On-line Error Detection in PV-Systems, in European Photovoltaic Solar Energy Conference and Exhibition, 17th, 1995.
- [3] Jennings C. PV module performance at PG&E, in Conference Record of the Twentieth IEEE Photovoltaic Specialists Conference, 1988, 1225–1229 vol.2.

- [4] French RH, Podgornik R, Peshek TJ, Bruckman LS, Xu Y, Wheeler NR, Gok A, Hu Y, Hossain MA, Gordon DA, Zhao P, Sun J, Zhang G-Q. Degradation science: Mesoscopic evolution and temporal analytics of photovoltaic energy materials, *Curr. Opin. Solid State Mater. Sci.*, 2015, 19, 212–226.
- [5] Peshek TJ, Fada JS, Hu Y, Xu Y, Elsaeiti MA, Schnabel E, Köhl M, French RH. Insights into metastability of photovoltaic materials at the mesoscale through massive I–V analytics, *J. Vac. Sci. Technol. B, Nanotechnol. Microelectron. Mater. Process. Meas. Phenom.*, 2016, 34, 50801.
- [6] Hu Y, Gunapati VY, Zhao P, Gordon D, Wheeler NR, Hossain MA, Peshek TJ, Bruckman LS, Zhang G-Q, French RH. A Nonrelational Data Warehouse for the Analysis of Field and Laboratory Data From Multiple Heterogeneous Photovoltaic Test Sites, *IEEE J. Photovoltaics*, 2017, 7, 230–236.
- [7] Wu Y-K, Chen C-R, Abdul Rahman H. A Novel Hybrid Model for Short-Term Forecasting in PV Power Generation, *Int. J. Photoenergy*, 2014, 2014, 1–9.
- [8] Jordan DC, Deline C, Johnston S, Rummel SR, Sekulic B, Hacke P, Kurtz SR, Davis KO, Schneller EJ, Sun X, Alam MA, Sinton RA. Silicon Heterojunction System Field Performance, *IEEE J. Photovoltaics*, 2018, 8, 177–182.
- [9] Ransome S, Sutterlueti J. Determining the causes and rates of PV degradation using the Loss Factors Model (LFM) with high quality IV measurements, in PV Performance and Monitoring Workshop, 2016.
- [10] Trupke T, Pink E, Bardos RA, Abbott MD. Spatially resolved series resistance of silicon solar cells obtained from luminescence imaging, *Appl. Phys. Lett.*, 2007, 90, 93506.
- [11] Peike C, Hoffmann S, Hülsmann P, Thaidigsmann B, Weiß KA, Koehl M, Bentz P. Origin of damp-heat induced cell degradation, *Sol. Energy Mater. Sol. Cells*, 2013, 116, 49–54.
- [12] Silverman TJ, Deceglie MG, Sun X, Garris RL, Alam MA, Deline C, Kurtz S. Thermal and Electrical Effects of Partial Shade in Monolithic Thin-Film Photovoltaic Modules, *IEEE J. Photovoltaics*, 2015, 5, 1742–1747.
- [13] Luo W, Khoo YS, Hacke P, Naumann V, Lausch D, Harvey SP, Singh JP, Chai J, Wang Y, Aberle AG, Ramakrishna S. Potential-induced degradation in photovoltaic modules: a critical review, *Energy Environ. Sci.*, 2017, 10, 43–68.
- [14] Kerr MJ, Cuevas A, Sinton RA. Generalized analysis of quasi-steady-state and transient decay open circuit voltage measurements, *J. Appl. Phys.*, 2002, 91, 399.
- [15] Chavali RVK, Li J V., Battaglia C, De Wolf S, Gray JL, Alam MA. A Generalized Theory Explains the Anomalous Suns–VOC Response of Si Heterojunction Solar Cells, *IEEE J. Photovoltaics*, 2017, 7, 169–176.
- [16] Kratochvil JA, Boyson WE, King DL. Photovoltaic array performance model., Albuquerque, NM, and Livermore, CA, 2004.
- [17] PV_LIB Toolbox. [Online]. Available: https://pvpmc.sandia.gov/applications/pv_lib-toolbox/.

- [18] NREL. National Solar Radiation Data Base, 2010. [Online]. Available: http://rredc.nrel.gov/solar/old_data/nsrdb/.
- [19] Zhao B, Sun X, Alam MA, Khan MR. Purdue University Meteorological Tool. [Online]. Available: <https://nanohub.org/resources/pumet>.
- [20] Jordan DC, Kurtz SR. The Dark Horse of Evaluating Long-Term Field Performance—Data Filtering, IEEE J. Photovoltaics, 2014, 4, 317–323.
- [21] Hejri M, Mokhtari H, Azizian MR, Ghandhari M, Soder L. On the Parameter Extraction of a Five-Parameter Double-Diode Model of Photovoltaic Cells and Modules, IEEE J. Photovoltaics, 2014, 4, 915–923.
- [22] Siemens Solar Panels Installation Guide. [Online]. Available: http://iodlabs.ucsd.edu/dja/codered/engineering/procedures/solarPower/siemens_solar_panels.pdf.